ACS Sustainable Chemistry & Engineering

pubs.acs.org/journal/ascecg

Research Article

# Next-Generation High-Performance Bio-Based Naphthalate Polymers Derived from Malic Acid for Sustainable Food Packaging

Ting-Han Lee, Huangchao Yu, Michael Forrester, Tung-ping Wang, Liyang Shen, Hengzhou Liu, Jingzhe Li, Wenzhen Li, George Kraus, and Eric Cochran*

Cite This: *ACS Sustainable Chem. Eng.* 2022, 10, 2624−2633

Read Online

ACCESS | Metrics & More | Article Recommendations | Supporting Information

**ABSTRACT:** Increasing demand for safe, convenient, and affordable packaging has prompted tremendous growth in single-use plastics, with attendant increases in carbon dioxide emissions and environmental waste. This study presents a family of engineering polyesters featuring biobased naphthalate rigid segments. The proposed polyesters can serve as an eco-friendly substitute for existing packaging materials, such as poly(ethylene terephthalate) (PET). Bio-PET analogs using 2,7-naphthalate-based rigid segments of dimethyl 1,2,3,4-tetrahydronaphthalene-2,7-dicarboxylate (THN) or dimethyl 2,7-naphthalene dicarboxylate (2,7-N) were synthesized via transesterification with ethylene glycol to the bis-hydroxy ester followed by polycondensation. The proposed bionaphthalate polyesters provide unique performance advantages. In experiments, the glass transition temperature of poly(ethylene THN) was comparable to that of PET ($T_g$ = 67.7 °C), and the glass transition temperature of poly(ethylene 2,7-N) was far higher ($T_g$ = 121.8 °C). The thermal stability of poly(ethylene 2,7-N) far exceeded that of PET, as evidenced by its char yield of 33.4 wt % at 1000 °C. Moreover, the poly(ethylene 2,7-N) also produced 30% less acetaldehyde under typical processing temperatures at 250−300 °C. Finally, the oxygen permeability values of these naphthalate-based polymers were less than $P_{O_2}$ = 0.0034 barrer, which represents a 3-fold improvement over PET (0.0108 barrer). Overall, biobased naphthalate rigid segment polyesters are promising candidates for sustainable packaging materials, particularly those requiring high gas barrier performance.

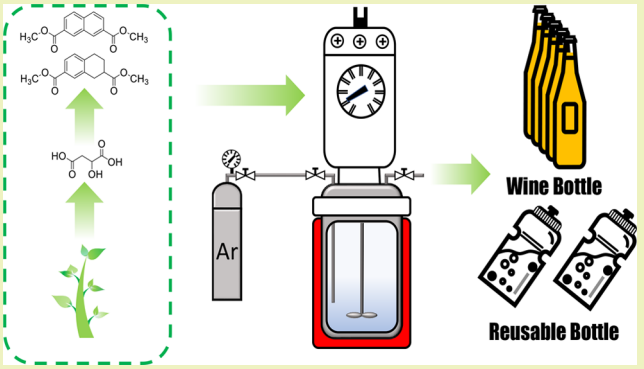


**KEYWORDS:** *Biobased naphthalate, High-performance bioplastics, Thermal stability, Barrier-enhanced, Green materials*



## INTRODUCTION

The advent of single-use plastics (SUPs) has heralded an age of convenience featuring easy long-term storage and widespread accessibility to food and drink.[1,2] However, the use of nondegradable petroleum-derived plastics has been a plague to the environment.[3,4] Poly(ethylene terephthalate) (PET) is an engineering thermoplastic with excellent thermal and chemical resistance as well as superb mechanical properties; however, the production of PET has a profound impact on the environment.[5,6] In 2015 alone, PET production was responsible for 137 million metric tons of greenhouse gas (GHG) emissions, which has resulted in significant consequences on climate and the environment.[7−9] Furthermore, PET performs poorly as a thermal and oxygen barrier in applications involving bottle reuse and liquor storage. PET can neither withstand deformation due to hot water cleaning nor impede the penetration of oxygen into the container, which can affect the flavor of the contents.[10,11] Consequently, academia and industry alike are seeking to overcome these issues through the development of high-performance biobased plastics from inexpensive and renewable feedstocks.[12] A number of materials have already made it to market, including polylactic acid (PLA), polybutylene succinate (PBS), and polyhydroxyalkanoates (PHAs); however, they cannot match the performance of PET.[13,14]

PET comprises a soft segment of ethylene glycol (EG) and a rigid segment of terephthalic acid (TPA). EG can be derived from renewable biomass resources; however, researchers have yet to develop a bioderived pathway to economically obtain TPA at industrial scales.[15] Therefore, researchers look toward other bioderived chemicals as alternatives. One likely substitute for TPA in aromatic polymers such as PET is 2,5-furandicarboxylic acid (FDCA), which has been identified by the US Department of Energy (DOE) as one of the top-12

Received: October 2, 2021
Revised: February 3, 2022
Published: February 16, 2022

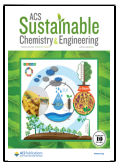







https://doi.org/10.1021/acssuschemeng.1c06726
*ACS Sustainable Chem. Eng.* 2022, 10, 2624−2633

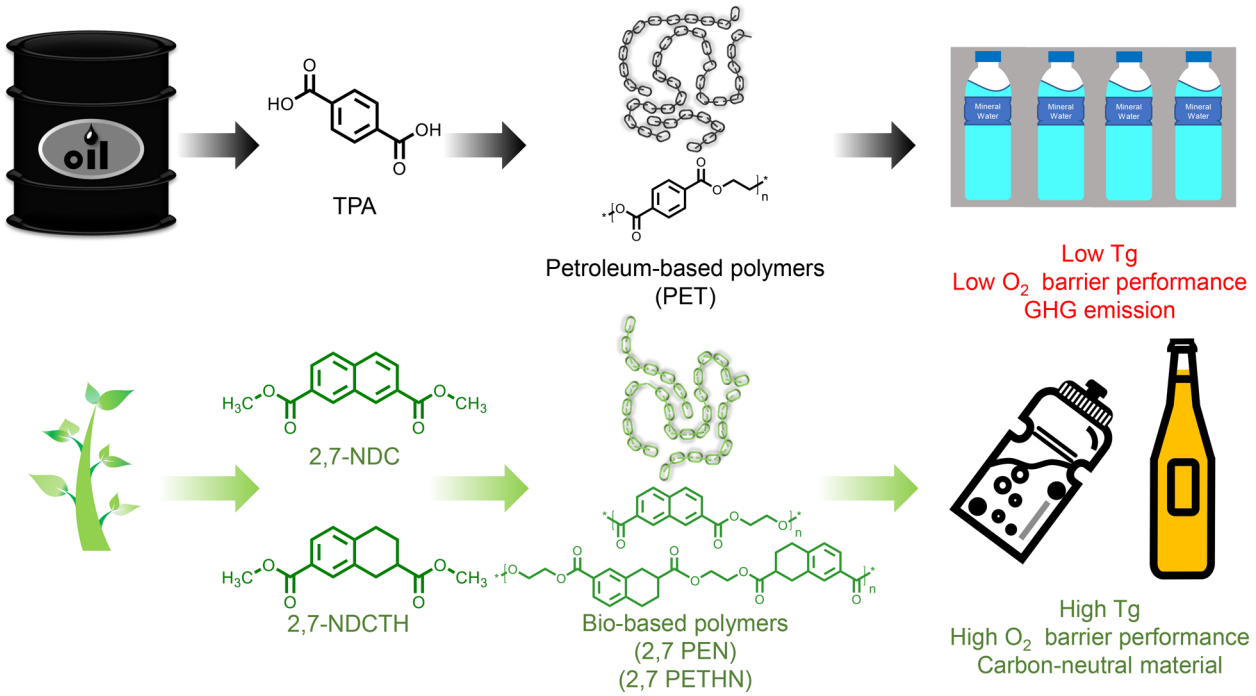


**Figure 1.** Conceptual illustration of bionaphthalate-based polymers for high-performance applications.

value-added chemicals derived from biomass.[16−19] In fact, a number of manufacturers, such as DuPont and DSM, have referred to FDCA as a "sleeping giant".[20] Numerous researchers investigating the substitution of TPA with FDCA have reported that the resulting materials outperform PET and other petroleum-derived plastics in many key areas, such as thermal and barrier aspects.[21−26] Nonetheless, discoloration is one of the major problems in furan-based polymers, owing to impurities, side reactions during high processing and reaction temperature, and the presence of catalyst and additives.[27]

Other bioderived TPA-like molecules with unique performance-advantaged properties have been developed. Yu and Kraus recently reported the preparation of dimethyl 1,2,3,4-tetrahydronaphthalene-2,7-dicarboxylate (THN) and dimethyl naphthalene-2,7-dicarboxylate (2,7-N) from malic acid (another DOE top-12 value-added chemical).[28] Considering the low yield and high cost of naphthalate-based monomers derived from petrochemical resources, this represents an important breakthrough. This approach also opens the door to the production of monomers and corresponding polymers with diverse properties. These bionaphthalate materials are considered an alternative to TPA, and in fact, the petroleum-derived 2,6-naphthalene dicarboxylate has been examined and shown to impart much better thermal and barrier properties than TPA-based plastics.[29,30] 2,6 PEN (poly(ethylene 2,6-naphthalate)) has been shown to outperform PET in almost every metric; however, its applicability is limited by its high cost, difficulties in obtaining the constituent monomers, and environmental concerns. Researchers have demonstrated through simulation and experiments that gas diffusivity can be reduced by adopting meta-substitution as an alternative to para-substitution on the benzene ring.[10,31,32] In commercial applications, PET has been modified by replacing a portion of the TPA with isophthalic acid (IPA) to improve barrier performance.[33] Therefore, polymers derived from 2,7-naphthalates could outperform 2,6-naphthalates in terms of barrier performance, which means that they could potentially access markets beyond the scope of PET, such as reusable bottles and UV-resistant packaging.[29,34] Finally, biobased 2,7-naphthalates are considered environmentally friendly.

As shown in Figure 1, to establish a bridge between poor-performance bioplastics and high-performance petroleum-based engineering thermoplastics, our strategy was introducing a new family of biobased polymers. This study investigated the use of biorenewable chemicals (e.g., 2,7-naphthalates) as hard segments in novel high-performance polymers, with a particular focus on the thermodynamic, dynamic, and mechanical properties. We selected THN and 2,7-N as candidate materials, due to their meta-substitution and fused ring systems, which can enhance thermal and barrier performance. We synthesized new naphthalate-based polymers via a conventional two-step polycondensation reaction in which the bis-hydroxy ester of the molecule was produced and then subsequently polymerized under high temperature and vacuum. We then analyzed the polymers to determine their chemical structure and molecular weight. Finally, we examined the effect of two different 2,7 molecules on thermal performance, crystallization, mechanical properties, and barrier characteristics.

## RESULTS AND DISCUSSION

Tables 1 and 2 and Figure 2 respectively summarize the chemical and thermal/mechanical properties of the polymers produced in this study.

The polymers were produced using a two-step process similar to that used in the industrial production of PET. The first step involved converting the diacid/dimethyl ester into the bis-hydroxy ester via esterification or transesterification, respectively. The ratio between diacid/dimethyl ester and EG was 1:10 and the conversion of diacid/diester precursors into bis-hydroxy ester monomers increased to 99% within 5 h without any side reaction (see Figures S8 and S9 of the


https://doi.org/10.1021/acssuschemeng.1c06726
ACS Sustainable Chem. Eng. 2022, 10, 2624−2633

**Table 1. Compositions and Characteristics of PET and Naphthalate-Based Polymers**

| sample code | polycondensation temp./time[a] (°C/h) | IV[b] (dL/g) | $M_n$[c] (kDa) | $M_w$[d] (kDa) | $Đ$[e] |
|---|---|---|---|---|---|
| PET | 240/8 | 0.73 | 16.3 | 27.2 | 1.67 |
| 27PEN[f] | 240/3 | 0.48 | 11.9 | 42.9 | 3.61 |
| 27PETHN[g] | 240/2.5 | 0.41 | 8.1 | 59.4 | 7.30 |
| PEI[h] | 240/8 | 0.55 | 23.4 | 37.3 | 1.59 |
| 26PEN | 240/6 | 0.75 | 24.0 | 43.2 | 1.80 |

[a]The esterification/transesterification reaction was carried out at 220 °C for 5 h and bis-hydroxy ester monomer comversion of each precursor is ≥99%, which was determined by gas chromatography–mass spectrometry. [b]Intrinsic viscosity was measured in phenol/1,1,2,2-tetrachloroethane (60/40, v/v) solution using an Ubbelohde viscometer at 25 °C. [c]Number-average molecular weight. [d]Weight-average molecular weight. [e]Dispersity calculated by $M_w/M_n$. The molecular weights were determined by GPC in 1,1,1,3,3,3-hexafluoro-2-propanol solution with Poly(methyl methacrylate) (PMMA) standards. [f]Poly(ethylene 2,7-naphthalate). [g]Poly(ethylene 2,7-tetrahydronaphthalate). [h]Poly(ethylene isophthalate).

Supporting Information, SI). Following the completion of monomer preparation and distillation to remove excess EG, the bis-hydroxy ester was mixed with an additional catalyst and converted into polyester with intrinsic viscosity (IV) values of >0.4 dL/g. The structural composition was confirmed by NMR and FTIR (see Figures S4 and S5). It should be noted that even though the melting point of 2,7-PEN is higher than polymerization temperature, the extent of crystallinity formed during reaction was too low to prevent mechanical stirring. This contrasts starkly with polymers like PET that develop sufficient crystallinity, even at the early stages of polymerization, to preclude agitation for temperatures above $T_m$. Nonetheless, viscosity was higher during the polymerization of poly(ethylene 2,7-N)(2,7-PEN) and much higher during the polymerization of poly(ethylene THN)(2,7-PETHN), far exceeding the viscosity of conventional PET polymerization. Thus, this reduced the reaction time, which limited the growth of polymer chain as determined by the IV and GPC results presented in Table 1. Interestingly, the dispersity ($Đ$) of 2,7-PEN and 2,7-PETHN far exceeded that typically associated with a polycondensation material (3.6 and 7.3, respectively). It is likely that the increase in viscosity during the reaction caused the increase in $Đ$ due to mass transport limitations. Further optimization of reaction conditions, including the use of plasticizers to reduce the melt viscosity, will be considered in future works. Despite the higher $Đ$ values, the molecular weights and IVs of the biopolymers were within the range typical of industrially produced PET, and well within the conditions required to assess the performance of these materials.

It is known that 2,6-PEN and poly(ethylene isophthalate)-(PEI) are commercially available comonomers used for the production of high-performance PET as well as PET drinking bottles and food packaging.[35,36] Note however that the existence of a naphthalene group and a meta-substitution structure within the polymer chains can disrupt the formation of a coherent crystal structure.[37,38] Thus, we expected that 2,7-PEN and 2,7-PETHN would have a similar (or perhaps more pronounced) effect on crystallinity, due to their meta- (as opposed to para-) substitution and fused ring system. We used temperature-controlled WAXS to observe both the crystallinity and the crystallization behavior as a function of temperature. Samples of each polymer were prepared via injection molding in a mold held at 270 °C, followed by rapid quenching to 40 °C. It should be noted that 2,7-PEN can be injection molded below its melting temperature due to the low extent of crystallinity. In other words, its primarily amorphous domains afforded melt-like processability in spite of the presence of small crystallites present below the melting point. Some of the samples were then annealed at 175 °C for 6 h for comparison against directly quenched samples; this temperature was chosen as a common intermediate temperature between $T_g$ and $T_m$ to provide both chain mobility and driving force for crystallization. All samples (unannealed and annealed) were tested at room temperature, as shown in Figure 3. After annealing, the para-substituted polymers (i.e., 2,6-PEN and PET) presented strong scattering peaks over a range of $11.5° \leq 2\theta \leq 32.8°$, in agreement with the results of previous studies,[38,39] whereas PEI and 2,7-PEN presented weaker scattering peaks. These results indicate that meta-substitution in conjunction with additional aromatic and cycloalkyl rings in PEI and naphthalate-based polymers disrupt crystallization.[40] Note that before annealing, 2,7-PEN presented scattering peaks over a range of $14° \leq 2\theta \leq 26.7°$, indicating that the material was soft enough for injection molding but was not in a molten state. Thus, it appears that the melting point of 2,7-PEN is higher than 270 °C as supported by the high temperature WAXS data. As shown in Figure 3, when the material was heated beyond 335 °C, the scattering peaks disappeared. We therefore conclude that the melting point is between 325 and 335 °C. In addition to a high melting point, we observed that 2,7-PEN underwent slow crystallization. WAXS analysis revealed no scattering peaks after the materials cooled to room temperature. This is in line with the DSC results. Note that this result was not unexpected given the stiffness and nonlinear axis of the fused aromatic rings. Unlike PET, it appears that 2,7-PEN did not have enough mobility for

**Table 2. Thermal Transition Properties of PET and Naphthalate-Based Polymers**

| | DSC | | | DMA | | TGA | | |
|---|---|---|---|---|---|---|---|---|
| sample code | $T_g$[a] | $\Delta H_m$[a] | $T_m$[a] | $T_\alpha$[b] | $T_\gamma$[b] | $T_{d,5\%}$[c] | $T_{d,max}$[c] | $R_{1000}$ (wt%)[c] |
| PET | 69.7 | 46.1 | 237.8 | 71.4 | −74.2 | 401.4 | 442.7 | 16.7 |
| 27PEN | 120.1 | 5.6 | 341.0 | 124.3 | −71.3 | 407.3 | 444.3 | 33.4 |
| 27PETHN | 67.3 | N.D.[e] | N.D. | 71.0 | −88.4 | 404.5 | 449.6 | 11.1 |
| PEI | 51.3 | N.D. | N.D. | N.A.[d] | N.A. | 393.3 | 445.9 | 12.5 |
| 26PEN | 114.6 | 1.6 | 245.1 | N.A. | N.A. | 413.6 | 446.6 | 31.3 |

[a]Glass transition ($T_g$) and melting ($T_m$) temperatures. The enthalpies ($\Delta H_m$) corresponded to the thermal transition. [b]Alpha transition temperature ($T_\alpha$) and gamma transition temperature ($T_\gamma$). [c]$T_{d,5\%}$: decomposition temperatures at which the weight loss reached 5% of its initial weight. $T_{d,max}$: the temperature at the maximum rate of decomposition. $R_{1000}$: the residual mass at 1000 °C. [d]Not available. [e]Not detected by DSC.



https://doi.org/10.1021/acssuschemeng.1c06726
ACS Sustainable Chem. Eng. 2022, 10, 2624−2633

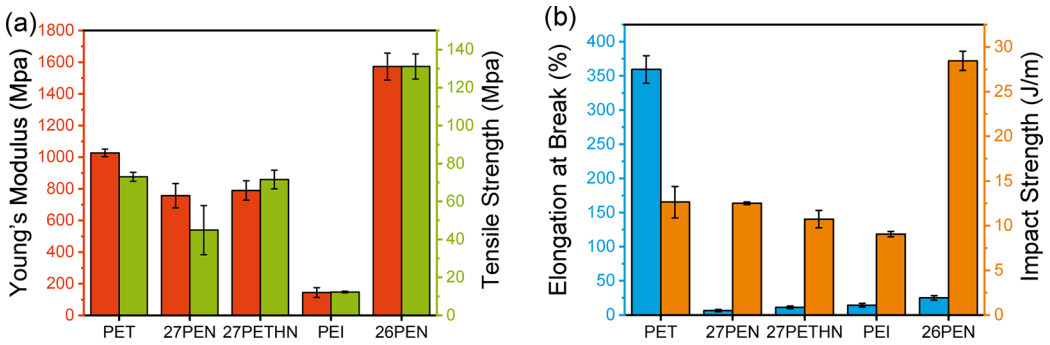


**Figure 2.** Tensile properties of PET and naphthalate-based polymers: (a) Young's modulus and tensile strength; (b) impact strength and elongation at break.

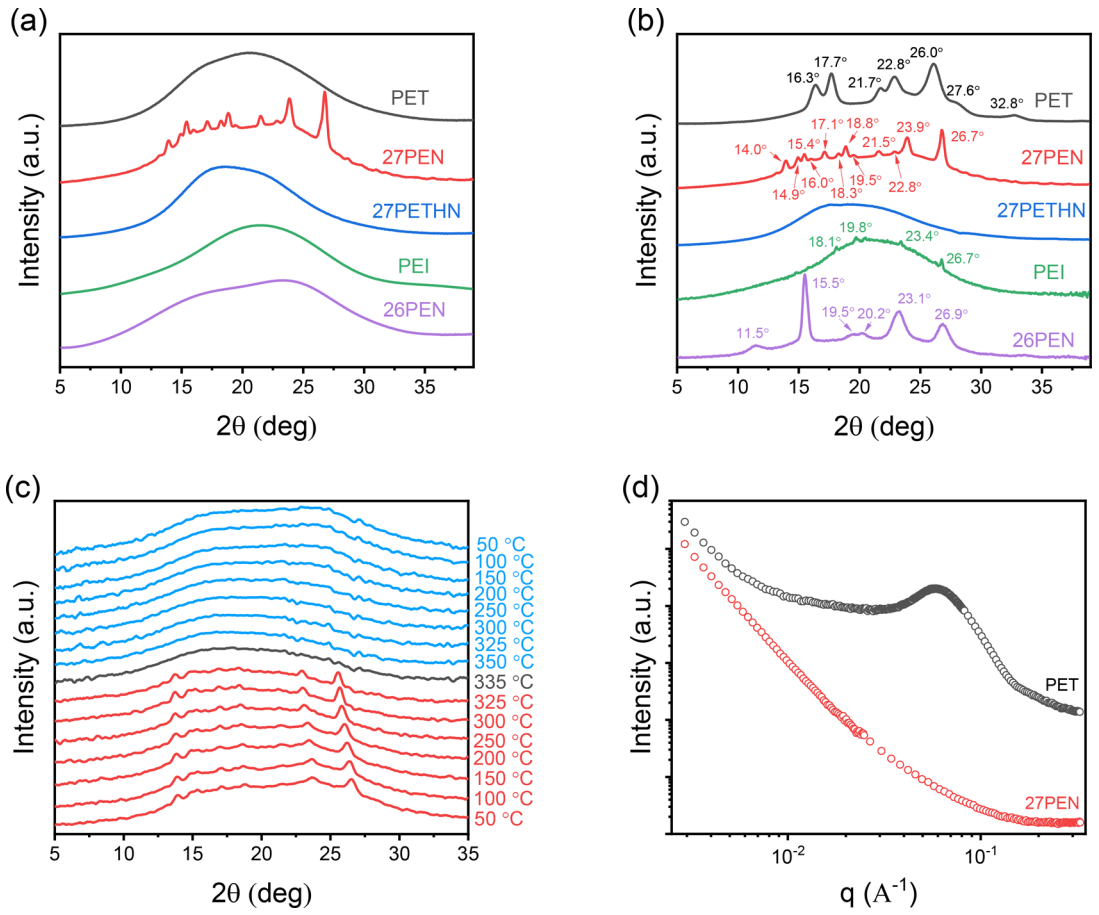


**Figure 3.** WAXS patterns of PET and naphthalate-based polymers: (a) tensile bar quenched from 270 °C; (b) after annealing at 175 °C for 6 h; (c) temperature-dependent WAXS of 2,7-PEN; and (d) SAXS spectra of PET and 2,7-PEN after annealing at 175 °C for 6 h.

rapid crystallization under the same condition. In the case of 2,7-PETHN, the samples presented no indications of crystallinity after annealing, indicating that it is an amorphous material. This can be attributed to the same mechanism affecting the structure of 2,7-PEN; however, the cycloalkyl ring in 2,7-PETHN has a more pronounced effect on the rearrangement of crystals. Finally, we investigated the crystal structure morphology of the biopolymers using SAXS to elucidate the effect of meta-substitution naphthalene ring in the 2,7-PEN polymer chain, and contrast it against the para-direction benzene ring of PET (see Figure 3). The peak obtained from PET sample indicates that the crystalline and amorphous domains were packed within a laminar structure, like a multilayer sandwich. Nonetheless, the lack of peak in the SAXS spectra of 2,7-PEN sample indicates that the arrangement of the crystal lattice differs from that of PET. This can perhaps be attributed to the random distribution of crystal structures among a predominantly amorphous domain, like chocolate chips dispersed in a cookie.

To further elucidate the thermal properties of the materials, DSC was performed (see Figure 4 and Table 2). The glass transition temperature of 2,7-PEN was 50 °C higher than that of PET and close to that of 2,6-PEN. Note that here the DSC results agreed with the DMA results. These high deformation temperatures of naphthalate-based polymers can be attributed to the stiff naphthalene ring in the polymer chains. Moreover,


https://doi.org/10.1021/acssuschemeng.1c06726
ACS Sustainable Chem. Eng. 2022, 10, 2624−2633

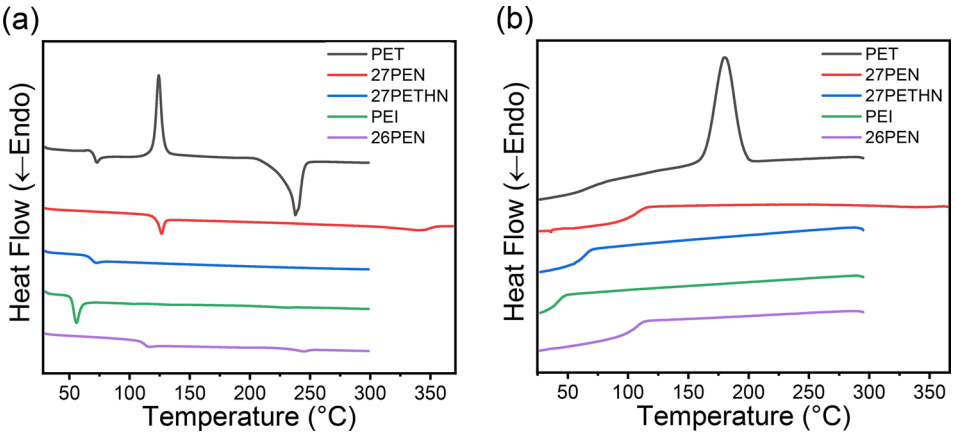


**Figure 4.** DSC thermograms of quenched PET and naphthalate-based polymers at scan rate of 10 °C min$^{-1}$: (a) heating and (b) cooling.

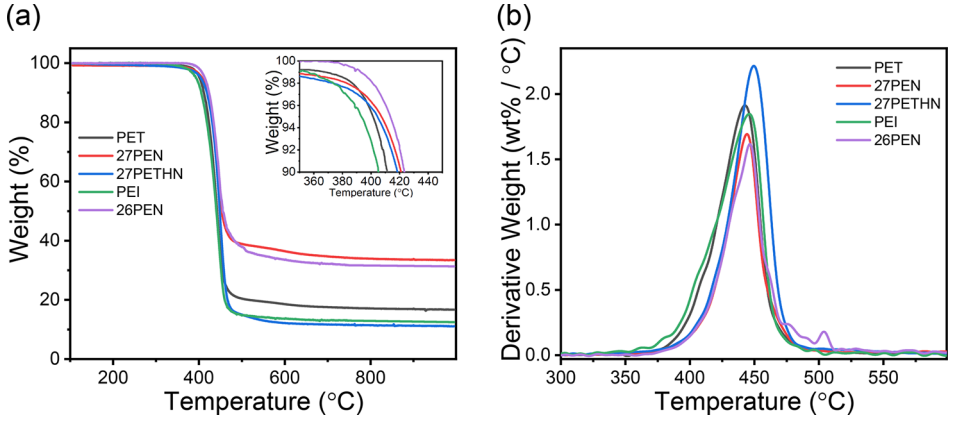


**Figure 5.** (a) TGA thermograms and (b) DTG curve of PET and naphthalate-based polymers with heating rate of 10 °C min$^{-1}$.

the melting temperature of 2,7-PEN was more than 100 °C higher than that of PET, which suggests that the presence of fused aromatic rings increased the amount of energy required to break the ordered crystal structure into disordered amorphous domains. As observed in the temperature-dependent WAXS patterns and DSC thermograms, 2,7-PEN did not undergo crystallization within short time scales and its melting enthalpy was significantly lower than that of conventional PET. This indicates that the crystallization behavior of 2,7-PEN is significantly less extensive than that of PET, due to a stiff naphthalene ring and nonlinear meta-substitution structure. The same phenomena have been observed in 2,6-PEN and PEI.[34,41] In the case of 2,7-PETHN, the WAXS and DSC results provided no evidence of 2,7-PETHN crystallization or melting. Also, its glass transition was close to that of PET (see Figure 4), due to the opposing effects of the additional cycloalkyl ring: on the one hand, the cycloalkyl ring increases the repeating unit mass, leading to a corresponding increase in $T_g$. On the other hand, the flexibility of the cycloalkyl ring decreases packing efficiency, placing downward pressure on $T_g$. Thus the opposing bulkiness and flexibility effects roughly cancel each other out, resulting in similar 2,7-PETHN and PET $T_g$ values.

The thermal properties of 2,7-PEN and 2,7-PETHN show considerable promise for a wide range of practical applications. Additionally, we performed experiments to characterize the thermal stability of the materials. On the one hand, the TGA results shown in Table 2 and Figure 5 indicate that the thermal stability of 2,7-PETHN was similar to that of PET, while producing slightly less char residue and slightly higher $T_{d,max}$ and $T_{d,5\%}$ values. On the other hand, 2,7-PEN produced nearly twice as much char residue as PET, with slightly higher $T_{d,max}$ and $T_{d,5\%}$ values. Unsurprisingly, the higher aromatic content in 2,7-PEN and 2,6-PEN had a significant effect in terms of improving thermal stability.[42] The $T_{d,5\%}$ of 2,7-PETHN was slightly higher than that of PET; however, the char yield was somewhat lower, likely due to the easily oxidized and burned cycloalkyl ring.[43]

These thermal properties suggest interesting possibilities for end-uses. The high melting point, glass transition, and thermal stability characteristics of 2,7-PEN (akin to that of petroleum-derived 2,6-PEN) would be well-suited to applications requiring high temperature stability, such as reusable and hot-filled bottles. By contrast, 2,7-PETHN could perhaps be used to produce highly amorphous fibers for textiles requiring flame-retardant and high resistance to thermal deformation. Confirming the applicability of these materials requires further analysis to elucidate the mechanical properties. The results of Instron and IZOD analysis are presented in Figure 2. The Young's modulus, tensile strength, and impact strength of 2,7-PEN and 2,7-PETHN were similar to those of PET; however, the elongation at break of 2,7-PEN was 60× less than that of PET and the elongation of 2,7-PETHN was 30× less. PET presents strain-hardening behavior, which tends to increase the Young's modulus and extend elongation prior to breaking. This can be attributed to strain-induced crystallization and the ability to distribute strain across the span of the testing section. In the case of 2,7-PETHN, the reduced elongation at break is


https://doi.org/10.1021/acssuschemeng.1c06726
ACS Sustainable Chem. Eng. 2022, 10, 2624−2633

likely caused by two factors: first, 2,7-PETHN is amorphous, resulting in poor mechanical properties in the absence of reinforcing entanglements. This follows the trend of PEI, which also does not show strain-induced crystallization and shows the attendant brittle performance.[44] Second, it is likely that the disparity between the nature of the aromatic ring and the cycloalkyl ring decreases weak bonding such as van der Waals force, which results in the resistance of entanglement between each of the rigid segments in the polymer chains, thereby reducing the number of entanglement sites. Overall, these factors decrease the ability of the material to stretch prior to breaking. The brittleness of 2,7-PEN may be due to the dispersion of crystal domains throughout the samples as well as the slow crystallization. In order to push 2,7-PEN into the completely amorphous state, a higher temperature condition without degrading the material would be required.[45]

SEM images of fractured polymer were analyzed with the aim of further elucidating the differences in mechanical properties. These images are presented in Figure 6. We

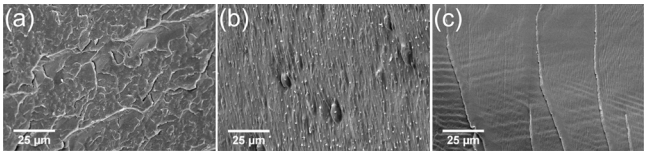


**Figure 6.** Fractured surfaces of PET and naphthalate-based polymers: (a) PET; (b) 2,7-PEN; and (c) 2,7-PETHN.

observed a striking difference between the samples. The PET samples presented a massive network of cracks with similar orientation across the specimen surface, indicating the ability of this material to dissipate energy throughout the sample. 2,7-PEN presented a surface that appeared as a collection of small crystals, indicating the semicrystalline nature of this material. As in the SAXS result, the crystals were randomly distributed throughout the amorphous phase. 2,7-PETHN presented a smooth surface with few fissures and a glossy appearance attributable to an entirely amorphous morphology. The absence of surface cracks on 2,7-PEN and 2,7-PETHN revealed the brittle nature of these naphthalate-based polymers.

To further investigate how changes in chemical structure affect the physical properties, DMA was used to study the dynamic mechanical thermal behavior. Figure 7 presents the $\gamma$-relaxation (sub $T_g$). This transition provides insight into localized chain motion, such as the bending and stretching of methylene ester linkages, as well as phenyl ring-flip motion.[46,47] We also observed that the incorporation of mobility-enhancing or mobility-restricting monomers coincided with the regions associated with these transitions.[48] The fact that the $T_\gamma$ transition of 2,7-PEN was slightly higher than that of PET can be attributed to the restricted mobility imposed by the fused aromatic ring, while the slightly lower of $T_\gamma$ transition of 2,7-PETHN can be attributed to the enhanced flexibility provided by the cycloalkyl ring. In addition, the $\gamma$-relaxation peaks of 2,7-PEN and 2,7-PETHN were also significantly lower than those of PET. The reduction in $\gamma$ peak area can be attributed to the incorporation of a fused ring system.[33] Cycloalkyl rings provide advantages in terms of mobility; however, fused rings have fewer degrees of freedom,

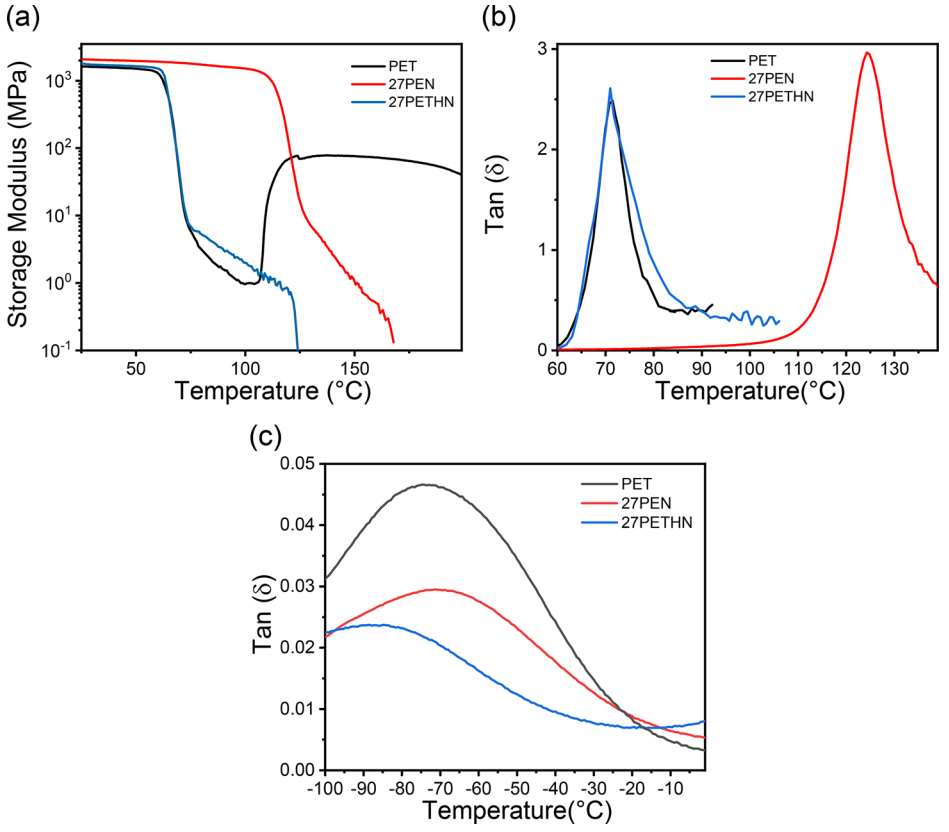


**Figure 7.** DMA spectra of PET and naphthalate-based polymers: (a) storage modulus; (b) tan ($\delta$) $\alpha$ relaxation transition; and (c) tan ($\delta$) $\gamma$ relaxation transition.



https://doi.org/10.1021/acssuschemeng.1c06726
ACS Sustainable Chem. Eng. 2022, 10, 2624−2633

which reduces the overall mobility of the chain. The reduction in $\gamma$ peak area can also be attributed to the meta-substituted structure of the functional groups.[10] The meta-naphthalene rings lack a linear axis of rotation; therefore, the ring-flip requires a cooperative motion of the neighboring ester and ethylene units. The angle of para-aromatic rings in PET does not impose this hindrance, and thus, shows the largest peak area.[22]

In addition to the $\gamma$-transition, the peak of the $\alpha$-transition (denoted as $T_\alpha$ in Figure 7) was comparable to the $T_g$ value of the polymers, as determined using DSC. The fact that the primary relaxation of 2,7-PEN exceeded that of PET indicates that the fused aromatic ring increased the rigidity of the polymer chain. The slightly lower primary relaxation of 2,7-PETHN can be attributed to an increase in the pliability provided by the cycloalkyl ring in the fused ring system, as shown in Figure 7. PET presented cold crystallization across a temperature range of 100−125 °C. This trend was not observed in 2,7-PEN or 2,7-PETHN. Considering the results from DSC and S/WAXS analysis, it appears that the crystalline domains dispersed in the amorphous phase of 2,7-PEN provide very little in the way of reinforcement. Under these conditions, the material behaved like a liquid, despite the presence of crystals in the sample. In the case of 2,7-PETHN, it simply presented poor crystallization ability.

In addition to the change in mechanical performance, Light et al. reported a significant correlation between the $\gamma$-relaxation peak area and oxygen diffusivity, an important property in many PET applications.[33] A reduction in the area of the $\gamma$-transition indicates that these materials may provide some advantage in terms of gas permeability. The results presented in Table 3 confirm the DMA findings, wherein 2,7-PEN was shown to reduce gas permeability by 80% and 2,7-PETHN reduced permeability by 70%. This is mainly attributable to the restricted ring-flip associated with the nonlinear axis of meta-naphthalene structure, which could suppress the motion of the chain related directly to gas diffusivity. However, not only the chemical structure, but also the polarity and free volume of the packaging materials could affect their barrier performance. In future studies, exploring these factors of the polymers more deeply would be interesting.

**Table 3. $O_2$ Barrier Characteristics and AA Content of PET and Naphthalate-Based Polymers**

| | | acetaldehyde (AA) content (mg/per kg polymer) | |
|---|---|---|---|
| sample code | $O_2$ permeability (Barrer)[a] | polymer powder | tensile bar |
| PET | 0.0108 | 85.7 | 119.2 |
| 27PEN | 0.0022 | N.D.[b] | 23.7 |
| 27PETHN | 0.0034 | 43.7 | 68.2 |
| 26PEN | 0.0077[c] | | |

[a]1 Barrer = $3.348 \times 10^{-16}$ mol m $m^{-2}$ $s^{-1}$ $Pa^{-1}$. [b]AA in specimen could not be detected by gas chromatographymass spectrometry. [c]Data cited from ref 29.

During the manufacture of food packaging materials, it is important to control the amount of acetaldehyde (AA) in plastic to prevent its leaching into the food and adding an unpleasant taste. High-temperature processing is required for manufacturing, which can cause thermal degradation to occur. Within a temperature range of 250 to 300 °C, hydroxyl groups at the chain terminus can attack the inner ester group, resulting in the formation of cyclic oligomers and subsequent degradation reactions to produce AA.[49] This thermal degradation mechanism is believed to be similar to that of 2,6-PEN.[42] However, 2,6-PEN is less susceptible to thermal degradation than is PET, due to the presence of naphthalene groups involved in the backbiting mechanism. It is reasonable therefore to assume that AA generation is probably lower in naphthalate-based polymers than in PET. The reduction in AA formation by 30% (see Table 3) illustrates that the thermal stability of naphthalate-based polymers exceeded that of PET during high-temperature processing. These results strongly suggest that the naphthalate-based polymers reported in this study are excellent candidates for a broad range of packaging applications.

## CONCLUSIONS

In this work, novel naphthalate-based polymers (2,7-PEN and 2,7-PETHN) derived from biomass were successfully synthesized by a two-step polycondensation reaction. The $T_g$ and $T_m$ values of 2,7-PEN were significantly higher than those of conventional PET. The $T_g$ value of 2,7-PETHN was similar to that of PET and $T_m$ was completely absent. WAXS and DSC analysis revealed that the crystallinity of 2,7-PEN was lower than that of PET and crystallization occurred more slowly, whereas 2,7-PETHN was highly amorphous. The mechanical stiffness and strength of 2,7-PEN and 2,7-PETHN are similar to those of PET; however, they are far more brittle. Interestingly, the thermal stability of 2,7-PEN and 2,7-PETHN is superior to that of PET, whereas the char yield shows an increase and a decrease to 2,7-PEN and 2,7-PETHN, respectively. Both materials provide significant advantages in terms of barrier performance and acetaldehyde formation.

2,7-PEN is suitable for applications requiring high resistance to thermal deformation and good barrier performance, as long as the mechanical properties are not crucial. 2,7-PETHN is applicable to applications requiring barrier performance superior to that of PET with lower processing temperatures, and good resistance to deformation. Furthermore, our biobased naphthalate polymers offer the potential of carbon neutrality since the $CO_2$ emitted in their production can be recycled by photosynthesis to produce biomass eventually, which has the advantage compared to petroleum-based PET. However, further end of life studies will be needed to provide a more comprehensive understanding of bionaphthalate-based polymers properties. Note that our research group is also currently engaged in copolymerizing these materials with PET, wherein we anticipate that they will reveal their true potential. Incorporation of 2,7-PEN with PET may allow for significant improvements in the melting point and thermal deformation/stability; moreover, the mechanical properties may even be tuned to show superior to those of PET homopolymer. This is like the results previously achieved via the inclusion of isophthalic acid in PET resins for plastic bottles and other food packaging. Finally, it appears that 2,7-PETHN could be used in applications requiring the suppression of crystallization. Given the improvements in permeability and acetaldehyde formation, these polymers are well-suited to the food packaging industry, and with further development, they could even be used to store wine, carbonated beverages, and food product for a longer period of time with fresh taste.



https://doi.org/10.1021/acssuschemeng.1c06726
ACS Sustainable Chem. Eng. 2022, 10, 2624−2633

## EXPERIMENTAL SECTION

**Materials.** Terephthalic acid (TPA, 99+%, Acros Organics), ethylene glycol (EG, anhydrous, 99.8%, Sigma-Aldrich),2,6-naphthalenedicarboxylic acid (2,6-NDA, 98+%, TCI America), and isophthalic acid (IPA, 99+%, TCI America) were used as precursors in polymer synthesis. Dimethyl naphthalene-2,7-dicarboxylate (2,7-N) and dimethyl 1,2,3,4-tetrahydronaphthalene-2,7-dicarboxylate (THN) were used as precursors for the synthesis of biobased polymers. They were synthesized from methyl coumalate through the Diels–Alder reaction as described in the SI in accordance with the procedures reported in the literature.[28] Zinc acetate ($Zn(CH_3COO)_2$), anhydrous, 99.8%, Alfa Aesar) and antimony(III) oxide ($Sb_2O_3$, 99%, Sigma-Aldrich) were respectively used as catalysts in the transesterification/esterification and polycondensation reactions. Triphenyl phosphate (TPP, > 99%, Sigma-Aldrich) was used as a thermal stabilizer in the polycondensation reaction. Solvents and chemical reagents for analysis, such as 1,1,1,3,3,3-hexafluoro-2-propanol (HFIP), dichloroacetic acid (DCAA), phenol, 1,1,2,2-tetrachloroethane, trifluoroacetic acid-d (TFA-d), and chloroform-d ($CDCl_3$), were purchased from Fisher Scientific and used as-received.

**Synthesis.** The synthesis of homopolymers was based on a classic two-step polycondensation reaction, as shown in Scheme S1. Two-step polymerization was performed in a stainless-steel reactor (Parr Instrument Company, type 4560). The first step involved the esterification/transesterification of TPA, IPA, 2,6-NDA, 2,7-N, or THN with EG using zinc acetate (0.15% molar ratio relative to diester) as the esterification/transesterification catalyst. No catalyst was used for TPA/IPA esterification because these chemicals served as reagent as well as catalyst.[50] Diacid/Diester and EG were charged into the autoclave reactor at a molar ratio of 1:10. After the system was purged for 30 min using argon, the reaction temperature was gradually increased to 220 °C and held at 110 psi for 5 h with an argon sweep to remove water/methanol. Agitation was performed using a stainless-steel impeller at 250 rpm. After the first step reaction, the monomer and excess EG were transferred to a round-bottom flask for the distillation of EG using an oil bath set to 110 °C under vacuum for 12 h. The monomer was then returned to the autoclave reactor using antimony(III) oxide (0.02% molar ratio relative to the diacid/diester) as a catalyst and triphenyl phosphate (0.1% molar ratio relative to the diacid/diester) as a thermal stabilizer. The second step of polycondensation to produce polymers was performed at 240 °C under high vacuum with the stirring speed set at 600 rpm. At the end of the reaction, the pressure was brought back to ambient pressure using argon gas to prevent thermal oxidation of the product. The polymers were then removed from the reactor to undergo drying under vacuum at room temperature for 24 h. The scale of one batch polymerization is approximately 50 g.

**Characterization.** Chemical structures were identified via solution $^1$H NMR using a Bruker Avance III 600 MHz spectrometer. $CDCl_3$ and Deuterated trifluoroacetic acid (75/25) were used at a concentration of 10 mg/mL in polymer sample preparation. Deuterated DMSO was used at a concentration of 10 mg/mL in precursor sample preparation.

Intrinsic viscosity was measured in a solvent mixture of phenol/1,1,2,2-tetrachloroethane (60/40 v/v) at 25 °C using a Ubbelohde viscometer (Xylem, type 537 13).

Molecular weight and dispersity were measured using a Tosoh Ecosec GPC (Tosoh Ecosec HLC-8320GPC) equipped with a UV and RI detector. HFIP and DCAA (50/50 v/v) were used to dissolve the samples at a concentration of 6 mg/mL. HFIP was used as the eluent at a flow rate of 0.3 mL/min. The molecular weights were determined relative to poly(methyl methacrylate) (PMMA) standards.

FTIR (iD7 ATR Accessory for the Nicolet iS 5 Spectrometer, ThermoFisher) was used to analyze functionality. Spectra were obtained from 4000 to 400 $cm^{-1}$ from 32 scans at a resolution of 4 $cm^{-1}$.

A Xenocs Xeuss 2.0 S/WAXS system with copper and molybdenum sources was used to estimate the extent of crystallinity, crystal structure morphology, and temperature response to crystallinity. Measurements were obtained using Mo K$\alpha$ as a light source under vacuum with the sample in an aluminum hermetic DSC pan. The specimens were fixed on a temperature-controlled stage (THMS600, Linkam Scientific) equipped with an LNP95 liquid-nitrogen cooling pump. Data acquisition was collected in intervals of 50, 25, 15, and 10 °C from room temperature at a heating/cooling rate of 30 °C $min^{-1}$. Each sample was equilibrated to the desired temperature for 300 s followed by acquisition for 600 s. Note that measurements obtained using Cu K$\alpha$ as a light source were performed under vacuum with the sample attached directly to the holder. The samples used in analysis were dumbbell-shaped tensile bars fabricated via injection molding. Data analysis was performed using Foxtrot 3.3.4 (SOLEIL Synchrotron, France) for absolute intensity correction of the background signal and the Irena macro running on Igor Pro for profile combination.[51] Crystallinity was calculated using Bragg's law (1) and Scherrer's eq 2, as follows:

$$\lambda = 2d \sin\theta \tag{1}$$

$$\tau = \frac{K\lambda}{\beta \cos\theta} \tag{2}$$

The thermal properties of the polymers were analyzed using differential scanning calorimetry (DSC, TA Instruments Q2500) under $N_2$ atmosphere. Samples (6–7 mg) were heated from 25 to 300 °C (2,7-PEN to 370 °C) at a rate of 10 °C $min^{-1}$, at which point they were held for 5 min before being cooled to 25 °C at a rate of 10 °C $min^{-1}$. Glass transition, crystallization, and melting temperature were obtained using Trios analysis software. The thermal stability of the polymers was estimated via simultaneous thermogravimetry/DSC (STA 449 F1 Jupiter, NETZSCH). In each experiment, 5–6 mg of the sample was heated in an alumina crucible under nitrogen from 40 to 1000 °C at a rate of 10 °C $min^{-1}$.

Tensile measurements were conducted using an Instron 3369 (load cell 1 kN; rate 10 mm-$min^{-1}$) using an ISO 527–2 1BB Dogbone (sample thickness: 2 mm, guage length: 10 mm) at room temperature. The impact strength was measured using an impact tester (Tinius-Olsen) according to ASTM D256 standards (sample dimension: 63.5 × 12.7 × 3 $mm^3$) at room temperature. The samples were prepared via injection molding (HAAKE Minijet, ThermoFisher) at 270 °C into a 40 °C mold.

The fractured surfaces of the samples were analyzed using a scanning electron microscope (SEM, Hitachi S4800 FE-SEM) at 10 kV SEM acceleration voltage. Note that the samples were immersed in liquid $N_2$ for 5 min before they were fractured.

Dynamic mechanical measurements were analyzed using rheometers (ARES-G2, TA Instruments) in torsion fixture mode with data obtained from −120 to 200 °C at a heating rate of 5 °C $min^{-1}$ with 0.1% strain at a frequency of 1 Hz.

Gas barrier performance was examined using an oxygen transmission rate analyzer (MOCON's OX-TRAN Model 2/21) in accordance with ASTM D3985 standards. Barrier specimens (sample thickness: 0.5 mm) were prepared via injection molding (HAAKE Minijet, ThermoFisher) at 270 °C into a 120 °C mold and quenched in cold water bath. The permeability of the films was measured via oxygen transmission at 23 °C under 1% relative humidity and 1 atm.[52,53]

The acetaldehyde (AA) content in the samples was quantified before and after injection molding using an Agilent 7890A equipped with an FID and a 5975C Mass Spectrometer (EI). The polymers were dissolved in a mixture of trifluoroacetic acid and chloroform (75:25, v/v), and then added dropwise into the methanol to precipitate the polyester, while the AA was retained in the methanol. Chromatographic separation was performed using a DB-WAX GC column.



https://doi.org/10.1021/acssuschemeng.1c06726
ACS Sustainable Chem. Eng. 2022, 10, 2624–2633

## ■ ASSOCIATED CONTENT

### Supporting Information

The Supporting Information is available free of charge at https://pubs.acs.org/doi/10.1021/acssuschemeng.1c06726.

Additional experimental details, including polymer synthesis pathway, IV analysis, GPC analysis, $^1$H NMR spectra, FTIR spectra, and mechanical tensile testing (PDF)

## ■ AUTHOR INFORMATION


### Corresponding Author

**Eric Cochran** − *Department of Chemical and Biological Engineering, Iowa State University, Ames, Iowa 50011, United States;* orcid.org/0000-0003-3931-9169; Email: ecochran@iastate.edu

### Authors

**Ting-Han Lee** − *Department of Chemical and Biological Engineering, Iowa State University, Ames, Iowa 50011, United States;* orcid.org/0000-0002-5531-052X

**Huangchao Yu** − *Department of Chemistry, Iowa State University, Ames, Iowa 50011, United States*

**Michael Forrester** − *Department of Chemical and Biological Engineering, Iowa State University, Ames, Iowa 50011, United States;* orcid.org/0000-0003-3063-9975

**Tung-ping Wang** − *Department of Chemical and Biological Engineering, Iowa State University, Ames, Iowa 50011, United States;* orcid.org/0000-0001-6292-3933

**Liyang Shen** − *Department of Chemical and Biological Engineering, Iowa State University, Ames, Iowa 50011, United States;* orcid.org/0000-0001-9928-2877

**Hengzhou Liu** − *Department of Chemical and Biological Engineering, Iowa State University, Ames, Iowa 50011, United States*

**Jingzhe Li** − *Department of Chemistry, Iowa State University, Ames, Iowa 50011, United States;* orcid.org/0000-0002-1856-1477

**Wenzhen Li** − *Department of Chemical and Biological Engineering, Iowa State University, Ames, Iowa 50011, United States;* orcid.org/0000-0002-1020-5187

**George Kraus** − *Department of Chemistry, Iowa State University, Ames, Iowa 50011, United States;* orcid.org/0000-0002-3037-8413

Complete contact information is available at: https://pubs.acs.org/10.1021/acssuschemeng.1c06726


### Notes

The authors declare no competing financial interest.

## ■ ACKNOWLEDGMENTS

The author thanks Sarah Cady (staff member at the ISU Chemical Instrumentation Facility) for training and assistance on the Bruker 600 MHz NMR. We would also like to thank Lucas Showman (staff member of the W. M. Keck Metabolomics Research Laboratory) for training and assistance on the Agilent GC-MS. Finally, we acknowledge financial support from the Center for Bioplastics and Biocomposites, DMR-1626315.

## ■ REFERENCES


(1) Chen, Y.; Awasthi, A. K.; Wei, F.; Tan, Q.; Li, J. Single-use plastics: Production, usage, disposal, and adverse impacts. *Sci. Total Environ.* **2021**, *752*, 141772.

(2) Sinha, V.; Patel, M. R.; Patel, J. V. PET waste management by chemical recycling: a review. *Journal of Polymers and the Environment* **2010**, *18*, 8−25.

(3) Joo, S.; Cho, I. J.; Seo, H.; Son, H. F.; Sagong, H.-Y.; Shin, T. J.; Choi, S. Y.; Lee, S. Y.; Kim, K.-J. Structural insight into molecular mechanism of poly (ethylene terephthalate) degradation. *Nat. Commun.* **2018**, *9*, 1−12.

(4) Thompson, R. C.; Olsen, Y.; Mitchell, R. P.; Davis, A.; Rowland, S. J.; John, A. W.; McGonigle, D.; Russell, A. E. Lost at sea: where is all the plastic? *Science* **2004**, *304*, 838−838.

(5) Hameed, M.; Bhat, R. A.; Singh, D. V.; Mehmood, M. A. *Innovative Waste Management Technologies for Sustainable Development*; IGI Global: Hershey, PA, 2020; pp 52−81.

(6) Al-Sabagh, A. M.; Yehia, F. Z.; Eshaq, G.; Rabie, A. M.; ElMetwally, A. E. Greener routes for recycling of polyethylene terephthalate. *Egyptian Journal of Petroleum* **2016**, *25*, 53−64.

(7) Zheng, J.; Suh, S. Strategies to reduce the global carbon footprint of plastics. *Nature Climate Change* **2019**, *9*, 374−378.

(8) Goyal, S.; Lin, F.-Y.; Forrester, M.; Henrichsen, W.; Murphy, G.; Shen, L.; Wang, T.-p.; Cochran, E. W. Glycerol Ketals as Building Blocks for a New Class of Biobased (Meth) acrylate Polymers. *ACS Sustainable Chem. Eng.* **2021**, *9*, 10620−10629.

(9) Forrester, M.; Becker, A.; Hohmann, A.; Hernandez, N.; Lin, F.-Y.; Bloome, N.; Johnson, G.; Dietrich, H.; Marcinko, J.; Williams, R. C.; et al. RAFT thermoplastics from glycerol: a biopolymer for development of sustainable wood adhesives. *Green Chem.* **2020**, *22*, 6148−6156.

(10) Polyakova, A.; Liu, R.; Schiraldi, D.; Hiltner, A.; Baer, E. Oxygen-barrier properties of copolymers based on ethylene terephthalate. *J. Polym. Sci., Part B: Polym. Phys.* **2001**, *39*, 1889−1899.

(11) Yoshida, S.; Hiraga, K.; Takehana, T.; Taniguchi, I.; Yamaji, H.; Maeda, Y.; Toyohara, K.; Miyamoto, K.; Kimura, Y.; Oda, K. A bacterium that degrades and assimilates poly (ethylene terephthalate). *Science* **2016**, *351*, 1196−1199.

(12) Paek, K. H.; Im, S. G. Synthesis of a series of biodegradable poly(butylene carbonate-co-isophthalate) random copolymers derived from CO2-based comonomers for sustainable packaging. *Green Chem.* **2020**, *22*, 4570−4580.

(13) Guidotti, G.; Soccio, M.; Lotti, N.; Gazzano, M.; Siracusa, V.; Munari, A. Poly (propylene 2, 5-thiophenedicarboxylate) vs. Poly (propylene 2, 5-furandicarboxylate): Two examples of high gas barrier bio-based polyesters. *Polymers* **2018**, *10*, 785.

(14) Zhu, Y.; Romain, C.; Williams, C. K. Sustainable polymers from renewable resources. *Nature* **2016**, *540*, 354−362.

(15) Ren, H.; Qiao, F.; Shi, Y.; Knutzen, M. W.; Wang, Z.; Du, H.; Zhang, H. Plantbottle™ packaging program is continuing its journey to pursue bio-mono-ethylene glycol using agricultural waste. *J. Renewable Sustainable Energy* **2015**, *7*, 041510.

(16) Werpy, T.; Petersen, G. *Top Value Added Chemicals from Biomass: Volume I−Results of Screening for Potential Candidates from Sugars and Synthesis Gas*; Report, 2004.

(17) Bozell, J. J.; Petersen, G. R. Technology development for the production of biobased products from biorefinery carbohydrates−the US Department of Energy's "Top 10" revisited. *Green Chem.* **2010**, *12*, 539−554.

(18) Liu, H.; Lee, T.-H.; Chen, Y.; Cochran, E. W.; Li, W. Paired electrolysis of 5-(hydroxymethyl) furfural in flow cells with a high-performance oxide-derived silver cathode. *Green Chem.* **2021**, *23*, 5056−5063.

(19) Liu, H.; Lee, T.-H.; Chen, Y.; Cochran, E.; Li, W. Paired and Tandem Electrochemical Conversion of 5-(Hydroxymethyl) furfural Using Membrane-Electrode Assembly-Based Electrolytic Systems. *ChemElectroChem.* **2021**, *8*, 2817−2824.

(20) van Putten, R.-J.; Van Der Waal, J. C.; De Jong, E.; Rasrendra, C. B.; Heeres, H. J.; de Vries, J. G. Hydroxymethylfurfural, a versatile platform chemical made from renewable resources. *Chem. Rev.* **2013**, *113*, 1499−1597.
(21) Hwang, K.-R.; Jeon, W.; Lee, S. Y.; Kim, M.-S.; Park, Y.-K. Sustainable bioplastics: Recent progress in the production of bio-building blocks for the bio-based next-generation polymer PEF. *Chem. Engi. J.* **2020**, *390* (12463), 124636.
(22) Burgess, S. K.; Leisen, J. E.; Kraftschik, B. E.; Mubarak, C. R.; Kriegel, R. M.; Koros, W. J. Chain mobility, thermal, and mechanical properties of poly (ethylene furanoate) compared to poly (ethylene terephthalate). *Macromolecules* **2014**, *47*, 1383−1391.
(23) Fei, X.; Wang, J.; Zhu, J.; Wang, X.; Liu, X. Biobased Poly (ethylene 2, 5-furancoate): No longer an alternative, but an irreplaceable polyester in the polymer industry. *ACS Sustainable Chem. Eng.* **2020**, *8*, 8471−8485.
(24) Zhu, J.; Cai, J.; Xie, W.; Chen, P.-H.; Gazzano, M.; Scandola, M.; Gross, R. A. Poly(butylene 2,5-furan dicarboxylate), a Biobased Alternative to PBT: Synthesis, Physical Properties, and Crystal Structure. *Macromolecules* **2013**, *46*, 796−804.
(25) Thiyagarajan, S.; Vogelzang, W.; Knoop, R. J. I.; Frissen, A. E.; van Haveren, J.; van Es, D. S. Biobased furandicarboxylic acids (FDCAs): effects of isomeric substitution on polyester synthesis and properties. *Green Chem.* **2014**, *16*, 1957−1966.
(26) Gomes, M.; Gandini, A.; Silvestre, A. J. D.; Reis, B. Synthesis and characterization of poly(2,5-furan dicarboxylate)s based on a variety of diols. *J. Polym. Sci., Part A: Polym. Chem.* **2011**, *49*, 3759−3768.
(27) Wu, L.; Mincheva, R.; Xu, Y.; Raquez, J.-M.; Dubois, P. High molecular weight poly (butylene succinate-co-butylene furandicarboxylate) copolyesters: From catalyzed polycondensation reaction to thermomechanical properties. *Biomacromolecules* **2012**, *13*, 2973−2981.
(28) Yu, H.; Kraus, G. A. Divergent pathways to isophthalates and naphthalate esters from methyl coumalate. *Tetrahedron Lett.* **2018**, *59*, 4008−4010.
(29) Lillwitz, L. Production of dimethyl-2, 6-naphthalenedicarboxylate: precursor to polyethylene naphthalate. *Applied Catalysis A: General* **2001**, *221*, 337−358.
(30) Hine, P.; Astruc, A.; Ward, I. Hot compaction of polyethylene naphthalate. *J. Appl. Polym. Sci.* **2004**, *93*, 796−802.
(31) Pavel, D.; Shanks, R. Molecular dynamics simulation of diffusion of O2 and CO2 in amorphous poly(ethylene terephthalate) and related aromatic polyesters. *Polymer* **2003**, *44*, 6713−6724.
(32) Polyakova, A.; Connor, D.; Collard, D.; Schiraldi, D.; Hiltner, A.; Baer, E. Oxygen-barrier properties of polyethylene terephthalate modified with a small amount of aromatic comonomer. *J. Polym. Sci., Part B: Polym. Phys.* **2001**, *39*, 1900−1910.
(33) Light, R.; Seymour, R. Effect of sub-Tg relaxations on the gas transport properties of polyesters. *Polym. Eng. Sci.* **1982**, *22*, 857−864.
(34) Sadanobu, J.; Inata, H. *Science and Technology of Polymers and Advanced Materials*; Springer: New York, 1998; pp 141−151.
(35) Kosmidis, V. A.; Achilias, D. S.; Karayannidis, G. P. Poly (ethylene terephthalate) recycling and recovery of pure terephthalic acid. Kinetics of a phase transfer catalyzed alkaline hydrolysis. *Macromol. Mater. Eng.* **2001**, *286*, 640−647.
(36) Fermeglia, M.; Cosoli, P.; Ferrone, M.; Piccarolo, S.; Mensitieri, G.; Pricl, S. PET/PEN blends of industrial interest as barrier materials. Part I. Many-scale molecular modeling of PET/PEN blends. *Polymer* **2006**, *47*, 5979−5989.
(37) Hu, Y. S.; Hiltner, A.; Baer, E. Improving oxygen barrier properties of poly(ethylene terephthalate) by incorporating isophthalate. II. Effect of crystallization. *J. Appl. Polym. Sci.* **2005**, *98*, 1629−1642.
(38) Chen, C.-W.; Yang, Y.-H.; Lin, S.-C.; Rwei, S.-P.; Shyr, T.-W. Crystal Structure and Tensile Fracture Morphology of Poly(ethylene terephthalate)-co-poly(ethylene 2,6-naphthalate) Block Copolyesters and Fibers. *Ind. Eng. Chem. Res.* **2020**, *59*, 18717−18725.
(39) Font, J.; Muntasell, J.; Cesari, E. Poly (butylene terephthalate) poly (ethylene terephthalate) mixtures formed by ball milling. *Materials research bulletin* **1999**, *34*, 157−165.
(40) Shik Ha, W.; Chun, Y. K.; Soon Jang, S.; Mook Rhee, D.; Rae Park, C. Preparation of poly (ethylene terephthalate-co-isophthalate) by ester interchange reaction in the PET/PEI blend system. *J. Polym. Sci., Part B: Polym. Phys.* **1997**, *35*, 309−315.
(41) Lee, S.; Ree, M.; Park, C.; Jung, Y.; Park, C.-S.; Jin, Y.; Bae, D. Synthesis and non-isothermal crystallization behaviors of poly (ethylene isophthalate-co-terephthalate) s. *Polymer* **1999**, *40*, 7137−7146.
(42) Turnbull, L.; Liggat, J.; MacDonald, W. Thermal degradation chemistry of poly (ethylene naphthalate)−A study by thermal volatilisation analysis. *Polymer degradation and stability* **2013**, *98*, 2244−2258.
(43) Akovali, G. *Polymers in Construction*; iSmithers Rapra Publishing: Shawbury, 2005.
(44) Salem, D. Microstructure development during constant-force drawing of poly (ethylene terephthalate) film. *Polymer* **1998**, *39*, 7067−7077.
(45) Wellen, R.; Rabello, M. The kinetics of isothermal cold crystallization and tensile properties of poly (ethylene terephthalate). *J. Mater. Sci.* **2005**, *40*, 6099−6104.
(46) Boyer, R. Dependence of mechanical properties on molecular motion in polymers. *Polym. Eng. Sci.* **1968**, *8*, 161−185.
(47) Robeson, L.; Faucher, J. Secondary loss transitions in antiplasticized polymers. *Journal of Polymer Science Part B: Polymer Letters* **1969**, *7*, 35−40.
(48) Maxwell, A.; Monnerie, L.; Ward, I. Secondary relaxation processes in polyethylene terephthalate-additive blends: 2. Dynamic mechanical and dielectric investigations. *Polymer* **1998**, *39*, 6851−6859.
(49) Montaudo, G.; Puglisi, C.; Samperi, F. Primary thermal degradation mechanisms of PET and PBT. *Polymer degradation and stability* **1993**, *42*, 13−28.
(50) Reimschuessel, H. K. Poly (ethylene terephthalate) formation. Mechanistic and kinetic aspects of direct esterification process. *Industrial & Engineering Chemistry Product Research and Development* **1980**, *19*, 117−125.
(51) Ilavsky, J.; Jemian, P. R. Irena: tool suite for modeling and analysis of small-angle scattering. *J. Appl. Crystallogr.* **2009**, *42*, 347−353.
(52) Wang, T.-p.; Kang, D.-Y. Highly selective mixed-matrix membranes with layered fillers for molecular separation. *J. Membr. Sci.* **2016**, *497*, 394−401.
(53) Wang, T.-p.; Kang, D.-Y. Predictions of effective diffusivity of mixed matrix membranes with tubular fillers. *J. Membr. Sci.* **2015**, *485*, 123−131.


https://doi.org/10.1021/acssuschemeng.1c06726
*ACS Sustainable Chem. Eng.* 2022, 10, 2624−2633